PAPER

Check for updates

Optimization of PAHs oxidation from contaminated soil using modified nanoscale zero-valent iron combined with potassium permanganate

Xiaoshuang Sun, [ID] [a] Zongxin Ran,[a] Yuerong Wu,[a] Chengwei Zhong,[ab] Weiwei Zhu,[a] Hameed Hllah[a] and Jiang Yu [ID] *[abc]

A novel synergistic oxidation technology based on modified nanoscale zero-valent iron (nZVI) and potassium permanganate ($KMnO_4$) was developed for polycyclic aromatic hydrocarbons (PAHs) remediation in actual contaminated soil. In this study, three surfactants were used as dispersants to modify nZVI, including poly acrylic (PAA), sorbitan monolaurate (SPAN-20) and sugar esters (SE). The following parameters were studied to optimize the coupling oxidation process: dispersants/nZVI ratio, dosage of oxidant based on soil oxidation demand (SOD), amount of modified nanomaterials added in the coupling system. By using zeta potential, XRD, SEM, BET characterization methods, the results show that nZVI successfully coated with 5% PAA, 20% SE and 10% SPAN-20 have the best stability and mobility to effectively reduce the agglomeration effect. The conditions for treating PAH contaminated soil with the three best modified nanocomposites combined with $KMnO_4$ were studied. The optimal conditions were defined as [SE-nZVI] = 10% and [$KMnO_4$] = 40% SOD_{max} for 24 h at 25 °C. The synergistic oxidation process under these optimal conditions and the two unoptimized processes of $KMnO_4$ and nZVI-$KMnO_4$ degraded 85%, 58.9% and 62% of PAHs, respectively. This showed that the treatment effect of the optimized oxidation process was improved by 1.3–1.5 times. Further, by using gas chromatography-mass spectrometry (GC-MS), adsorption and electrophilic substitution reaction were speculated as the oxidation mechanism of PAHs treated by the coupling system of SE-nZVI-$KMnO_4$. PAHs could finally be decomposed into 9-methylene-9H-fluorene, fluoranthene and 1,5-diphenyl-1,4-pentadiyn-3-one and reached a safer status in the soil.

1. Introduction

Soil is one important sink of the organic pollutants polycyclic aromatic hydrocarbons (PAHs) during continuous development of industrialization, which stores more than 90% of the PAHs in the environment.[1] PAHs have the characteristics of low water solubility, high fat solubility, and difficult degradation, so they are easily adsorbed on particulate matter, and then transferred and accumulated in the soil medium. In addition, PAHs can also come from atmospheric sedimentation, sewage irrigation, and industrial wastewater discharge. Therefore, using an efficient method to remove PAH pollutants from soil has become a focus in the field of environmental remediation.

Chemical oxidation is widely used in research and practice of contaminated soil remediation due to its high treatment efficiency, relatively low treatment cost, and good applicability. Previous research results have found that the selection of oxidants is critical when treating PAHs contaminated sites soil with many different oxidants. As we know, activation of sodium persulfate requires strict reaction conditions and easily affects soil pH value. Hydrogen peroxide and Fenton reagents have low repair efficiency, and a large amount of heat has to release in the oxidation process, and also change the pH value of soil, which leads to secondary pollution problems. Potassium permanganate ($KMnO_4$) has good remediation ability on treating the PAHs soil, and few pollutants are volatilized into the surrounding environment during the oxidation process, which is beneficial to the environment. Considering the remediation efficiency and environmental risk of different oxidant treatments, $KMnO_4$ is a better oxidant choice. Chen studied the remediation effects of various oxidants on PAHs contaminated soil, finding that $KMnO_4$ degraded PAHs with the highest efficiency with reaching 94.06%.[2] Zhao *et al.* also found that when remediating PAHs contaminated sites, $KMnO_4$ showed the best performance with up to 96% PAHs removal.[1] The single oxidant with high stability,

[a] Department of Environmental Science and Engineering, College of Architecture and Environment, Sichuan University, No. 24 South Section 1, Yihuan Road, Chengdu, 610065, P. R. China. E-mail: yuj@scu.edu.cn

[b] Yibin Institute of Industrial Technology, Sichuan University, Yibin 644000, P. R. China

[c] Institute of New Energy and Low Carbon Technology, Sichuan University, Chengdu, 610065, P. R. China

but its oxidation intensity is low. Therefore, it is very necessary to improve the reaction activity of oxidants through thermal activation, photo-activation, and metal activation.

As an effective adsorbent and reducing agent, nanoscale zero-valent iron (nZVI, Fe^0) has attracted great attentions due to its small particle size, high surface activity, strong reducing potential, magnetic recovery property and environmental friendliness.[3] Compared with conventional zero-valent iron, nZVI has higher specific surface area and surface reaction activity, which makes it has unique advantages in the application of removing refractory pollutants and low-concentration pollutants. However, nZVI easily aggregates and is prone to be oxidized in air and water, leading to low reactivity in applications.[4,5] Numerous researchers have found that zero-valent iron nanoscale materials can effectively remove all kinds of inorganic and organic pollutants in soil, so they have a good market application prospect. The composite stabilizer of "galacturonic acid (GAM) – carboxymethyl cellulose (CMC)" was used to modify nZVI, and the fixed conversion rate of Cr(VI) in the chromium residue soil of the modified nZVI suspension system reached 97.55%.[6] A study which using nZVI combined with nano-bimetal (Fe/Cu) to treat chromium pollution in soil showed that the composite nano-material had a better degradation effect on water-soluble Cr(VI) in soil than the single nZVI, and the removal rate was as high as 97.77%.[7] In addition, nZVI has been widely used to treat the degraded soil organochlorine pollutants due to its good reductive dechlorination and molecular reactivity. For example, in the study of nZVI combined with microbial degradation of PCBs in soil, it was found that compared with single treatment systems, nZVI reduction dechlorination had a synergistic effect with microbial aerobic degradation, and the removal efficiency of PCBs was significantly high.[8] In general, nZVI and its modified materials are mostly used for inorganic heavy metals and organochlorine pollutants in soil. However, there are relatively few studies on persistent organic pollutants (POPs) such as PAHs with wide pollution range and high potential harm. In view of the problems of nZVI modification technology, such as less research amount and immature technology, it is still a hot topic of current academic research to explore nZVI modification technology with higher efficiency, stability and repair efficiency.

Hence, great effort is needed to solve the problem of the stability and dispersity of the nZVI-based materials. The modification of nZVI is currently a more effective means.[9,10] A large number of studies have shown that dispersants such as polymeric materials and surfactants can significantly improve the dispersibility and stability of nZVI, so that improving its removal efficiency on pollutants. He *et al.* modified nZVI with anionic surfactant polyacrylic acid (PAA), and found that the agglomeration of nZVI decreased, the shape of nZVI tended to be spherical, the particle size of nZVI was uniform and the specific surface area increased significantly.[11] Lin's study also showed that the addition of PAA can effectively prolong the suspension time of nZVI particles.[12] Wang used an anionic surfactant polyacrylamide (APAM) to modify the surface of nZVI, and the results showed that the stability and oxidation resistance of the modified nZVI particles were significantly improved.[13] In addition, dispersing agents such as

rhamnolipid (RL), carboxymethyl cellulose (CMC), and sodium oleate (NaOA) were used to modify the surface of nZVI, which finally obtained a stable and high pollutant removal rate material.[14–16] Generally, that coating the surface of nZVI particles with modified materials such as surfactants or high polymer can effectively prevent its oxidation. Meanwhile, the charge number on nZVI surface increases and the electrostatic repulsion between particles becomes stronger. Surface modification can not only improve the stability of nZVI, but also enhance its mobility. The coating material that can effectively reduce the agglomeration of nZVI particles needs to have these characteristics that it can interact with nanoparticles to prevent co-agglomeration, and will not cause secondary pollution to the environment, and it's cheap and readily available, and has good mobility and dispersion as well.[17]

Therefore, based on the advantages and disadvantages of current nZVI surface modification methods, we proposed a new methodology for synthesizing novel nanoscale zero-valent iron (nZVI) materials with superior properties by using three surfactants including an anionic surfactant (polyacrylic acid, PAA) and two less studied non-ionic surfactants (SPAN-20; sugar esters, SE). This study set out to use the best modified material to activate $KMnO_4$, forming a coupled oxidation system, and to investigate the degradation of PAHs in the actual contaminated site soil, and further to analyze its reaction process and mechanism, which try to propose a simpler nZVI modification method and an oxidation system that takes into account economy, safety, high efficiency, and large-scale usability. It is hoped that this research will contribute to provide new ideas and new directions for the two important areas of *in situ* chemical oxidation (ISCO) remediation of organic contaminated soil and the development of new nanomaterials.

2. Materials and methods

2.1 Soil sample preparation

The soil samples were collected from four corporate plant areas in Chengdu, China. The basic information and distribution of sampling points are shown in Table 1 and Fig. 1. Preparation of PAHs contaminated soil: take the same amount of soil samples from each of the four sites to prepare mixed soil samples. Weigh the appropriate amount of PAH standard solution and dissolve it in acetone, stir it evenly and pour it into a glass with a sufficient amount of mixed soil samples, so that the solvent can slowly and completely evaporate in the fume hood. PAHs are generally divided into three forms according to their properties and molecular weights, namely, low molecular weight PAHs (LMW PAHs) containing 2–3 rings, medium molecular weight PAHs (MMW PAHs) containing 4 rings, and high molecular weight PAHs (HMW PAHs) containing 5–6 rings. Use the prepared contaminated soil for subsequent experiments. The concentration of PAHs (TPAH: total PAH, LMW PAHs, MMW PAHs, HMW PAHs) were determined according to National Environmental Protection Standards of the People's Republic of China. The determination was repeated three times and the average value was used as the concentration of contaminated soil. Fig. 2 shows the contents and proportions of 16 PAHs detected in contaminated soil samples.

Table 1 Characteristics of the different soil sites

Number	Sampling site	Sampling point coordinate	pH value	Soil type	Characteristic organic pollutants
1	Lubricant plant (1)	(104°5′48″N, 30°45′4″E)	7.73–8.21	Clay/loamy clay	PAHs
2	Lubricant plant (2)	(104°5′30″N, 30°45′10″E)	5.89–8.22		
3	Asphalt plant (1)	(103°55′32″N, 30°23′56″E)	7.32–8.32		
4	Asphalt plant (2)	(104°16′35″N, 30°51′33″E)	7.03–8.19		

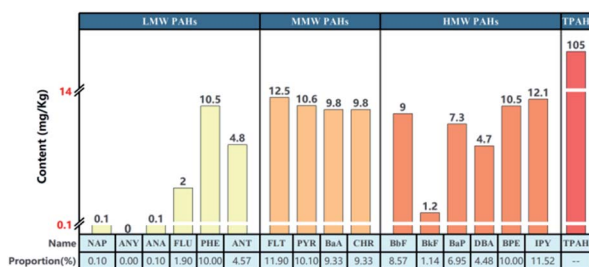**Fig. 1** Schematic diagram of research location and soil sampling site.

Fig. 2 Contents (proportion) and total detected values of 16 PAHs in contaminated soil samples.

2.2 Synthesis of nZVI and coated nZVI

Nano zero-valent iron (nZVI) was prepared by the traditional liquid-phase reduction method.[18] 200 mL of saturated $Fe_2(SO_4)_3$ solution is poured into a three-hole round bottom flask, and then high purity nitrogen is added into the solution for 10 min to remove dissolved oxygen. The excess $NaBH_4$ powder was dissolved in a 100 mL mixture of ethanol and water (v/v = 1 : 1), poured into the separating funnel, and then nitrogen was introduced for protection and mechanical stirring. Then the $NaBH_4$ solution was dropped into a three-hole round bottom flask at a constant and continued stirring for 10 min after titration. The black suspension in the reaction solution was

nZVI. Under the protection of nitrogen, the liquid part is removed by suction filtration, and the remaining black solid matter is collected in a brown reagent bottle with anhydrous ethanol, and the nZVI is evenly dispersed by ultrasound for 15 min. After nitrogen is injected into the top, it is sealed and stored in a refrigerator at 4 °C.[19]

Select Polyacrylic Acid (PAA), Sorbitan Monolaurate (SPAN-20) and Sugar Esters (SE) as dispersants, and set different mass ratios of dispersant/nZVI (w/w), the mixture ratio of PAA/nZVI was 0.05, 0.08, 0.1, 0.2 and 0.5, respectively; the mixture ratio of SPAN-20/nZVI was 0.01, 0.02, 0.05, 0.1 and 0.2, respectively; the mixture ratio of SE/nZVI was 0.01, 0.02, 0.05, 0.1 and 0.2, respectively. The prepared dispersants were added to $Fe_2(SO_4)_3$ solution separately under ultrasonic assisted vibration. Then the solution was fully stirred to make the mixture uniform. Thereafter, the coated nZVI was also prepared according to the above-mentioned synthesis method of nZVI. The molecular structures of the zero-valent iron coating process and the three surfactants (dispersants) are shown in Fig. 3.

2.3 Experimental methods

2.3.1 Optimization experiment of dispersant dosage. In this study, sedimentation spectroscopy was used to study the suspension properties of different nZVI materials, so as to
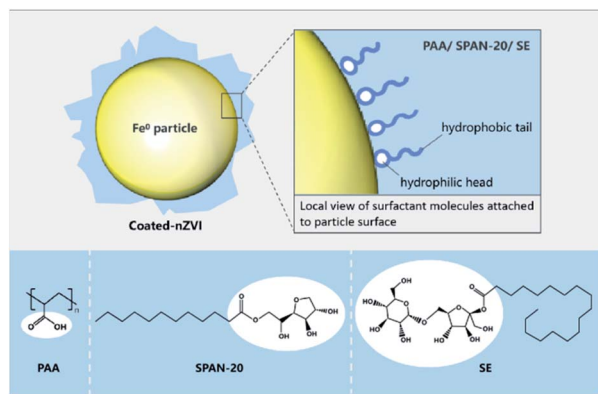
Fig. 3 Schematic diagram for the modification of nZVI with three surfactants.

compare and evaluate the dispersion differences of each material.[4] The 1 g L^{-1} nZVI suspension was under ultrasound for 20 min (25 °C, 40 kHz), then took out 4 mL of it and placed it in a glass cuvette, and scanned continuously for 2100 s at a wavelength of 508 nm in an ultraviolet-visible spectrophotometer (UV-6800A).

The penetration properties of nZVI with different dispersant contents were evaluated by the simulated string method.[16,20] Moisten 50 mL acid buret with distilled water, filled it with 2 cm glass beads ($d \approx 0.3$ cm) at the bottom, then added 15 cm quartz sand, and finally filled it with an appropriate amount of glass beads at the top to ensure stability of the column. Used a separatory funnel to drop 1 g L^{-1} nZVI suspension into the column at a uniform of 1–2 drops per second, collected the filtrate at 10, 20, 30, 40, 50, 60 min, respectively, and used the *o*-phenanthroline spectrophotometric method to determine the iron content in the filtrate and drawn a penetration curve.[21] Based on the results of the sedimentation spectrum and simulated column experiment, the migration performance of PAA, SPAN-20, and SE dispersants and the dosage at the best sedimentation performance were analyzed.

2.3.2 Determination of soil oxidant demand (SOD). KMnO$_4$ was selected as the oxidant, and the oxidant was mixed evenly with the soil samples at a dosage of 0.5 mM g^{-1}, 1 mM g^{-1} and 2 mM g^{-1}, respectively (soil/water = 1 : 5). The reaction was placed in a thermostatic shaker at 25 °C, 150 rpm for 3 h, and then placed in a dry place away from light for static reaction. After 24 h, 48 h, 96 h and 168 h reaction, soil-oxidant mixture samples were taken to analyze the residual oxidant and determine the optimal dosage of oxidant. This study took the soil oxidant demand (SOD) index to accurately assess the actual oxidant consumption of contaminated soil. SOD refers to the theoretical amount of oxidant added when the oxidant oxidizes the PAHs in soil to CO$_2$ and H$_2$O. SOD was determined according to the same method used by Yang *et al.*[22] The calculation method of SOD index is as follows:

$$\text{SOD}_t = \frac{V(C_0 - C_t)}{M_{\text{soil}}}$$

where, SOD$_t$ represents the demand for soil oxidant at time t; V: volume of oxidizer added before reaction (mL); C_0: the concentration (g mL^{-1}) of oxidizer added before the reaction; C_t: the concentration of oxidant (g mL^{-1}) after reaction time t; M_{soil}: the soil mass to the reaction system (g); SOD$_{\text{max}}$: the maximum oxidant demand of soil when SOD reaches equilibrium.

2.3.3 Optimization experiment of oxidant dosage. According to the experimental results in section 2.3.2, using the SOD index as the benchmark, the oxidant dosage of 20%, 40%, 60%, and 80% of SOD$_{\text{max}}$ was studied respectively for the oxidation effect of the PAHs in the tested soil, which was used for the optimization experiment of the oxidant application amount. Using a 250 mL Erlenmeyer flask as the reaction vessel, mix 20 g of the test soil (mixed soil samples from four sites) with 100 mL of KMnO$_4$ of different concentrations, and then place it in a COS-2112F constant temperature shaker (25 °C, 150 rpm) for 3 h, then place it in a dark place to react for 24 h, in which parallel experiments are set up for each treatment. The mixture of water and soil was centrifuged (4500 rpm) and washed, while the bottom was dried, ground, and sieved, and the contents of TPAH and 16 kinds of PAHs were determined.

2.3.4 Remediation experiment of nZVI coupled oxidation. According to the characterization results of the modified materials, three kinds of coated nZVI with the best effects, namely PAA, SE, and SPAN-20, were selected as the activation materials of KMnO$_4$. The bare/coated nZVI : KMnO$_4$ (w/w) concentration gradients were set as 1%, 5%, 10%, 20%, respectively. In addition, the application amount of KMnO$_4$ should be determined under the optimal removal efficiency of TPAH according to the results of the "oxidant application amount optimization experiment". Weigh 20 g of PAHs contaminated soil and add it into the triangle bottle, apply a certain amount of oxidant and activator, then react in dark for 24 h, take the mixture, centrifuge (4500 rpm) and discard the supernatant. Subsequent operations are the same as in section 2.3.3.

2.4 Analytical methods

2.4.1 Extraction and analysis of soil PAHs. Accelerated solvent extraction solid phase extraction (ASE-SPE) column was used to extract and purify PAHs from soil samples. 20 g soil sample, 5 g anhydrous sodium sulfate and 1 μg PAHs mixed standards were accurately weighed into stainless steel flushing tube. The mixture was extracted continuously with dichloromethane and acetone (1 : 1) in ASE 350 rapid solvent extractor (Dionex, USA). The extract was concentrated by automatic nitrogen blowing instrument (models 7910001, Labconco, USA), and then washed with *n*-hexane and concentrated 3 times. The concentrate was transferred to a solid-phase extraction column (Supelco, USA) and purified with a mixture of dichloromethane and *n*-hexane (1 : 1). After concentration by nitrogen blowing, acetonitrile was added for solvent conversion. Finally, the volume was accurately determined and transferred to the injection bottle.

PAHs in the sample will be quantitatively analyzed by an external standard method in high-performance liquid

chromatography (HPLC) (Agilent 1260). The chromatographic column is special for PAHs analysis (250 mm × 4.6 μm, Agilent, USA). The PAHs were determined by the HPLC with the following conditions: flow rate 0.8 mL min^{-1}, column temperature 30 °C, stopping time 45 min, the post-running time 5 min, and gradient elution with the mobile phase consisted of ultrapure water and acetonitrile.

2.4.2 Analysis of material properties. The zeta potential of each material in a pure water dispersion system was measured by a dynamic light scattering instrument (Malvern zs90, UK) to analyze its dispersion performance. The specific surface area (BET) of materials was determined by the traditional method (Brunauer–Emmett–Teller isotherm). Using aperture analyzer (Asap 2460, USA) to degass at 100 °C for 5 h (N$_2$ as adsorption medium, the sample density was 1.000 g cm^{-3}, and the tank temperature was −195.85 °C). The volume of nitrogen adsorbed by (bare/coated) nZVI material was measured under different pressures, and the specific surface area of the material was calculated by the isothermal adsorption equation.[5] X-ray diffraction (XRD) instrument (Bruker D8 ADVANCE, GER) was used to determine the crystal structure and composition of bare/coated nZVI particles.[5] Scanning electron microscope (SEM) instrument (Zeiss GeminiSEM 500, GER) was used to analyze the surface morphology and particle size of bare/coated nZVI particles.

The sample self-test repetition rate is controlled at 10%, and the *r*-value range of the 16 kinds of PAHs standard curve is 0.9995–0.9997, and the relative deviation of sample self-inspection is less than 30%. All data were analyzed by SAS and SPSS software.

3. Results and discussion

3.1 Property evaluation of bare/coated nZVI materials

3.1.1 Effects of surfactants. To explore whether using surfactants as dispersants to modify nZVI has an improvement effect, different proportions of PAA, SE, SPAN-20, and freshly prepared nZVI were mixed to prepare a suspension for sedimentation spectroscopy experiments and simulations column experiment.

Fig. 4(a–c) shows the penetration curves of the newly prepared nZVI and the nZVI modified by the three dispersants in different proportions. It can be seen that the penetration performance of the unmodified nZVI was poor. The total iron concentration in the filtrate only reached 49.3% of the original solution concentration at 60 min. The penetration of nZVI was improved to varying degrees after modification with different doses of dispersants. It showed that the migration of nZVI modified by dispersant was better than that of single nZVI. In this study, SPAN-20 improved the penetration of nZVI most significantly, and the filtrate concentration of different proportions of SPAN-20 coated nZVI reached more than 90% at 60 min. In addition, at 60 min, the filtrate concentration of the coated nZVI at a low dose of SPAN-20 (1%, 2%) and a medium dose of PAA (8%, 10%) reached the concentration of the original solution. The nZVI modified by PAA, SE, and SPAN-20 at the dosage of 0.1, 0.1, and 0.01 respectively showed the best penetration performance. The ability of different dispersants to improve the penetration performance of nZVI is that SPAN-20 was the best, but SE was the worst.
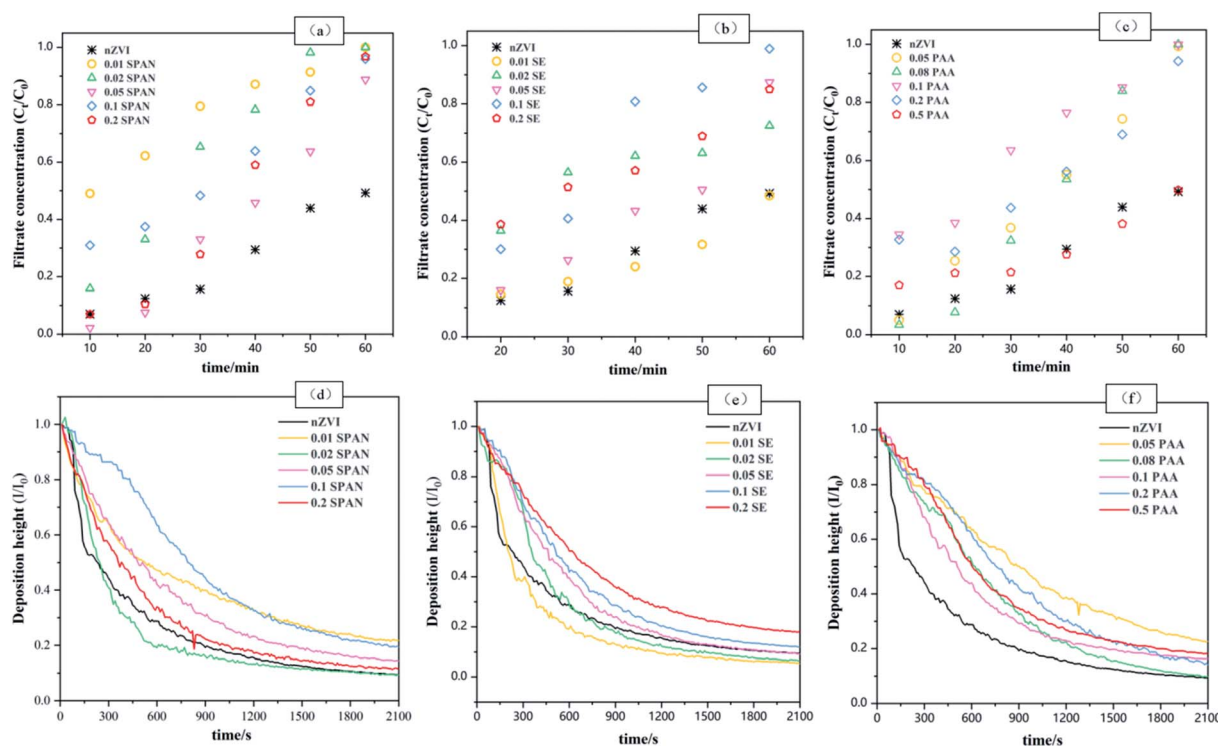

Fig. 4 (a−c): The influence curve of nZVI modified by SPAN-20 (a), SE (b) and PAA (c) on the migration of pipe string over time; (d−f): the influence curve of nZVI modified by PAA (a), SE (b) and SPAN-20 (c) on the suspension sediment thickness over time.

Fig. 4(d–f) shows the sedimentation spectrum curves of single nZVI and nZVI modified by different proportions of dispersants. The deposition height (I/I_0) of nZVI particles in suspensions of different materials decreased with time. The time point is stable at 2100 s, and the sedimentation performance showed obvious differences. Among them, the deposition height of unmodified nZVI decreased rapidly in a short time, which indicated that its stability was poor. After being modified by dispersants, the sedimentation rate of nZVI suspension decreased, which indicated that the surface modification of nZVI by PAA, SE, and SPAN-20 slowed down its aggregation effect in the dispersion system and enhanced its stability. Different dispersant dosages showed different effects on the settlement of nZVI. The low-dose PAA (5% applied amount) has the best modification effect on nZVI. With the increase of dispersant dosage, the agglomeration effect of materials increases, which is due to the bridging phenomenon of nZVI under a high dose of PAA, resulting in destroying the stability of colloid and reducing the suspension of particles.[23] SE and SPAN-20 had the best modification effect on nZVI under the conditions of high dose (20% applied amount) and medium dose (10% applied amount), respectively. This is because SPAN-20 is a polyol-type non-ionic surfactant, and SE is also a typical non-ionic surfactant. The interaction between abundant hydroxyl groups on its molecular surface makes its branched-chain extend outward, which strengthened the steric hindrance of molecules in the ring structure and improved the dispersion and stability of modified nZVI particles.[25] The deposition height (I/I_0) of PAA, SE, and SPAN-20 at 2100 s under the optimal dosage was 0.227, 0.179, and 0.144, respectively.

Combined with the sedimentation spectrum experiment and simulated string experiment, considering the settlement property, penetration property, dosage, and dispersant cost of nZVI, the 5% PAA, 20% SE and 10% SPAN-20 coated nZVI were selected for subsequent material characterization.

3.1.2 Characterization of modified nZVI

3.1.2.1 Stability of modified nZVI. The particles in a single nanoparticle dispersion system often have high activity. Due to the lack of other particles in the close pairing, there is a tendency of spontaneous interaction between the particles because of the nano-action energy,[24] which makes the nanoparticles have magnetic properties and induces them to agglomeration occurs in the solution. The zeta potential of particles can measure the mutual attraction or repulsion between particles, to quantify the stability of colloidal dispersion. Fig. 5(a) shows the zeta potential of nZVI modified by different dispersants in pure water dispersion without pH adjustment. The zeta potential value of single nZVI was 3.58. After the modification by 10% SPAN-20, 5% PAA, and 20% SE, the zeta potential of nZVI changed to 9.61, 9.49, and −13.0, respectively. 20% SE showed the greatest improvement on the zeta potential of nZVI, indicating that all the dispersants could significantly improve the stability of nZVI in the pure water dispersion system. Compared with SPAN-20, the SE molecule has a more stable ring structure and a more complex branched-chain, so it can improve the dispersion of nZVI more significantly. As for PAA, its positive electric properties improved the electrostatic repulsive force between particles, so that the PAA-modified nZVI particles have better dispersion. In conclusion, 10% SPAN-20, 5% PAA, and 20% SE can increase the steric hindrance/classical repulsion between nZVI particles and make the particles achieve better stability, so that they can migrate in the soil easily.
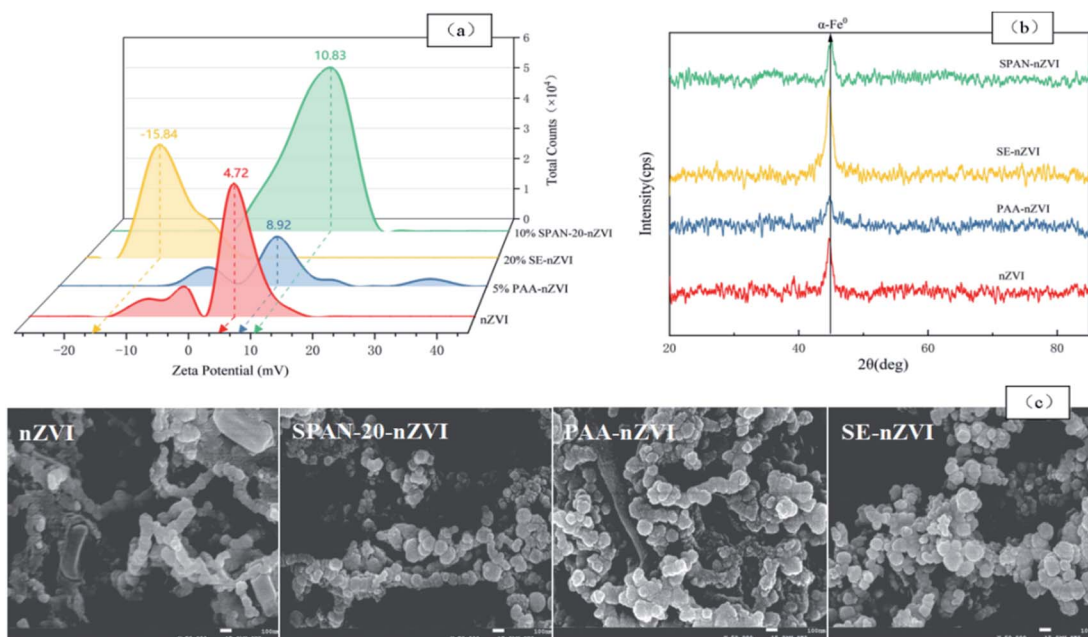

Fig. 5 (a): Zeta distribution data of (bare/coated) nZVI in pure water dispersion system; (b): XRD patterns of nZVI powders modified by different dispersants; (c): SEM analysis of (bare/coated) nZVI (×50 000).

3.1.2.2 Composition and chemical state. Fig. 5(b) shows the existence and crystal form of nZVI were identified by comparing the XRD characteristic peaks of different nZVI materials. The results show that different nZVI materials have obvious diffraction peaks at $2\theta = 44.7°$, corresponding to the diffraction peaks of α-Fe[0],[26] indicating that the presence of nZVI in the materials modified by the three dispersants is not affected. Among them, the diffraction peak corresponding to α-Fe[0] does not appear to be broadened, and the sharp peak is obvious, indicating that the modified nZVI showed a better crystalline structure.[27] After the modification, the α-Fe[0] diffraction peak height of the three nZVI materials decreased and the peak shape became dull, indicating that the crystallinity of nZVI after the modification treatment decreased. In addition, except for 20% SE-coated nZVI, the XRD spectra of 5% PAA and 10% SPAN-20 modified nZVI did not show obvious diffraction peaks at the 31.8° characteristic peak corresponding to Fe_3O_4, indicating that these two materials did not produce surface oxidation of nZVI,[13] that is, the coating property is good. As for the surface oxidation of the SE-coated nZVI, it is speculated that during the preparation of the SE-Fe_3O_4 mixture, the high concentration of SE forms a molecular film to hinder the flow of the liquid, so the foam in the liquid is stable that the oxygen in the foam causes the material part oxidation. The grain size of nZVI can be calculated by the Debye Scherrer formula:[28]

$$D_p = \frac{k\lambda}{B\cos\theta}$$

where D_p is the grain size/nm; k (Scherrer constant) = 0.89; λ (X-ray wavelength) = 0.154056; B is the diffraction peak half-height width/rad; θ is the diffraction angle/rad. According to this formula, the particle sizes of single nZVI and the three modified nZVI are calculated, and the results are shown in Table 2. According to the calculation results of the formula, the average grain size of the bare nZVI is 14.5 nm. After being modified by different dispersants, the average particle size of the particles increased. This also explained the reason why the diffraction peaks of the three modified nZVI materials in the XRD pattern narrowed to a certain extent, indicating that the surface of nZVI particles formed a stable coating layer after modification.

3.1.2.3 Morphologic structure and BET surface areas. Fig. 5(c) shows the characterization results by SEM to single nZVI and nZVI modified by 10% SPAN-20, 5% PAA, and 20% SE, respectively. The single nZVI particles are spherical, but the inter-particle agglomeration phenomenon is serious, and they are distributed in the shape of spheres and chains. After nZVI was coated with SPAN-20, the particles are still spherical, the surface is rougher than single nZVI, and the particle size is larger, which shows that the dispersant effectively forms a stable coating on the surface of nZVI particles. It shows that the modification reduced the agglomeration effect of nZVI to a certain extent. The SEM results of PAA-nZVI and SE-nZVI were similar.

In addition, after measuring and analyzing the specific surface area of nZVI materials before and after modification, the specific surface area of a single nZVI is 76.9 $m^2\ g^{-1}$, and different dispersant modification treatments showed different effects on the specific surface area of nZVI. The specific surface area of nZVI modified by 10% SPAN-20 was 77.8 $m^2\ g^{-1}$, which has no significant change compared to the unmodified nZVI. The 20% SE modification treatment reduced the specific surface area of nZVI to 65.5 $m^2\ g^{-1}$, presumably because the coating increased the particle size, thereby reducing the specific surface area. The 5% PAA modification treatment significantly increased the specific surface area of nZVI to 137.4 $m^2\ g^{-1}$. It is speculated that the surface of the coating is loose and the pore structure is developed, which makes the overall specific surface area of the material increase. The increased surface area can also play a positive role in the adsorption and degradation of pollutants in the soil.

3.2 Effects of nZVI-$KMnO_4$ on the degradation of PAHs in soil

3.2.1 Influence of $KMnO_4$ dose on the PAH degradation. In practice, adding excessive oxidizer blindly will increase the repair cost and cause economic burden. Therefore, the concept of the soil oxidant demand (SOD) index was used in this study. Considering that PAHs in soil is a mixture of multiple compounds with complex composition, it is difficult to obtain the dosage of oxidant directly through stoichiometric ratio. Therefore, specific SOD was obtained through experiments to accurately calculate the amount of oxidant. The experiment and calculation results of SOD in PAHs contaminated soil showed that: the consumption of SOD in soil was positively correlated with the initial concentration of $KMnO_4$. When the initial concentration of $KMnO_4$ was 1 mmol g^{-1}, the oxidant began to remain, that is, the dosage of the oxidant was in a sufficient state. When 1 mmol g^{-1} $KMnO_4$ was reacted for 7 days, SOD was basically stable, and SOD_{max} was 148.24 g $KMnO_4$ per kg soil. Based on the above results, based on SOD index, the oxidation effect of PAHs in tested soil was studied when the dosage of SOD_{max} was 20%, 40%, 60% and 80%, respectively.

The removal efficiency of TPAH in contaminated soil by adding $KMnO_4$ is shown in Fig. 6(a). Oxidation efficiency of $KMnO_4$ to TPAH increased firstly and then decreased with the increase of the $KMnO_4$ dose. It was found that the increase of oxidant dose could improve the degradation efficiency of PAHs in soil, because of the high concentration of oxidizer to promote its chemical reaction process to pollutants.[29] In this study, when the dosage of $KMnO_4$ increased from 20% SOD_{max} to 40% SOD_{max}, the removal efficiency of TPAH increased by 24.2%, while the removal efficiency of TPAH began to decrease as the oxidant further increased. It is speculated that the main reason is that high-concentration oxidants are rapidly consumed by organic matter,[30] which leads to a reduction in the dose involved in the oxidation reaction of pollutants. Moreover, high-

Table 2 Average grain sizes of nZVI and modified nZVI

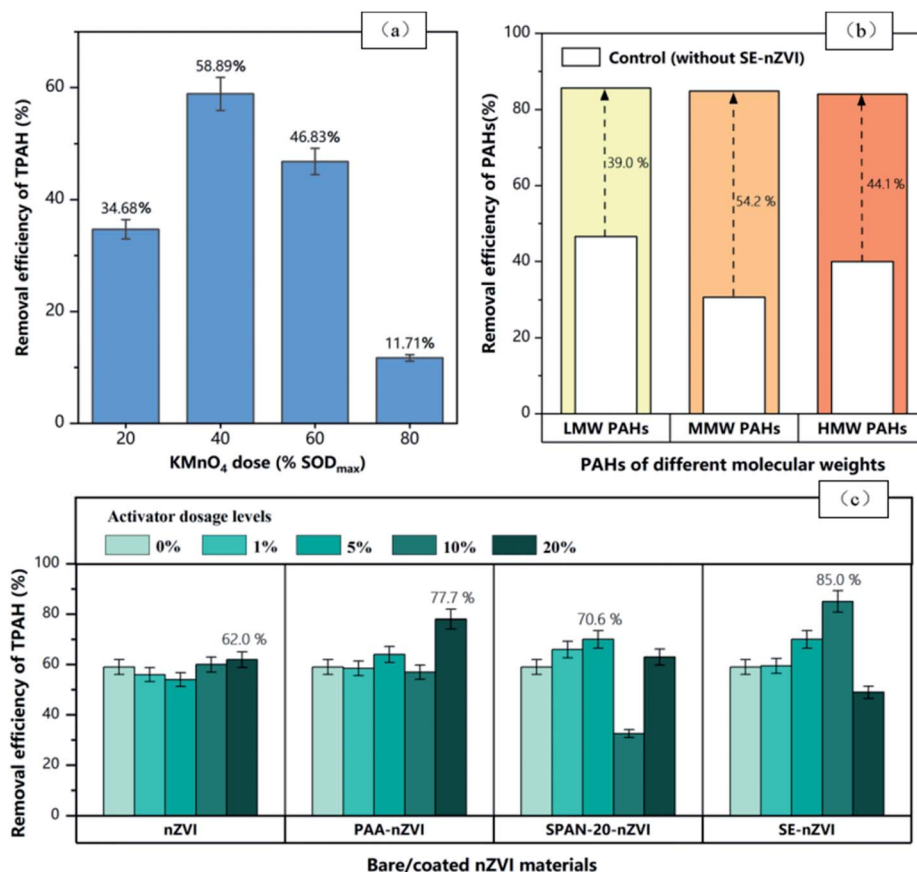| Parameters	nZVI	SP-nZVI	PAA-nZVI	SE-nZVI
$B/°$	0.718	0.591	0.665	0.641
B/rad	0.013	0.010	0.012	0.011
D_p/nm	14.524	17.645	15.682	16.269

Fig. 6 (a) Effects of different dosage of KMnO₄ on removal efficiency of on TPAH in soil; (b) 10% SE–nZVI combined with 40% SOD$_{max}$ KMnO₄ (optimal optimization system); (c) effect of different dosage of activators on removal efficiency of TPAH in soil.

concentration oxidants destroy the organic components of the soil, making the high-cyclic PAHs easily fixed by soil particles. PAHs adsorbed in the sub-micron or nanoscale pores of the soil are not easily desorbed from the soil particles or further oxidized and degraded due to strong hydrophobicity.[31] In addition, incomplete oxidation by the oxidant may cause the degradation of high-cyclic PAHs into low-cyclic or mid-cyclic PAHs, thereby leading to the removal efficiency of TPAH at a low level. The removal efficiency of KMnO₄ to TPAH under different dosage treatments is between 11.7% and 58.9%, which is similar to the results of Ferrarese et al.,[29] but it is different from the 78–99% results obtained by Liao et al.,[32] which may be caused by different soil properties.

Fig. 6(b) compares the removal efficiency of KMnO₄ to low/medium/high molecular weight PAHs (LMW/MMW/HMW) in the soil under optimal application conditions. The results show that when KMnO₄ is added at 40% SOD$_{max}$, the removal efficiency of LMW is 46.6%, while the removal efficiencies of MMW and HMW are 30.6% and 40.0%, respectively (as shown in the white bar of Fig. 6(b)), indicating that KMnO₄ is more effective in degrading LMW in the soil, which is similar to Cai's finding.[33] This is because LMW is more soluble in water than HMW, while HMW has more benzene rings, stronger hydrophobicity, complex and stable structure, and is easy to be adsorbed on sediments, so it has worse availability and is more difficult to be oxidized.[34,35]

Despite oxidizing the PAHs, KMnO₄ also has the characteristics of a slow reaction process and non-selectivity, and the manganese oxides such as MnO₂ produced by it may change the soil structure and affect the removal of pollutants.[36–38] Therefore, how to effectively control the reaction process of the KMnO₄ oxidation system needs to be further studied.

3.2.2 Different activators dosage impact analysis. According to the results of previous characterization experiments of single/coated nZVI, the best performance of coated nZVI containing PAA (5%), SE (20%) and SPAN-20 (10%) were selected as the activator of KMnO₄. Fig. 6(c) shows the removal efficiency of TPAH in soil by KMnO₄ combined with different dosage of bare/coated nZVI materials. KMnO₄ had .a high removal efficiency of TPAH when the amount of 40% SOD$_{max}$ was applied, and the removal efficiency was 58.89% after 24 hours of reaction. When adding 1% (bare) nZVI, the removal efficiency of TPAH did not increase significantly. When the dosage of the activator increased to 20%, the removal efficiency of TPAH showed a significant difference. Under the condition of KMnO₄, the removal efficiency of TPAH by bare nZVI increased slowly at first and then stabilized, while PAA-nZVI and SPAN-20-nZVI decreased first and then increased, on the contrary, SE-nZVI increased first and then decreased. The optimal TPAH removal efficiency of the four materials appeared in 20% nZVI (62.0%), 20% PAA-nZVI (77.7%), 5% SPAN-20-nZVI (70.6%), and 10% SE-nZVI (85.0%) treatments;

and compared with the control group without activator (only 40% SOD$_{max}$ KMnO$_4$), the removal efficiency of the four best groups increased by 5.3%, 31.9%, 19.9% and 44.4%, respectively. In addition, compared with the nZVI, the application of modified nZVI significantly improved the degradation efficiency of TPAH. When the doses of nZVI coated with PAA and SPAN-20 increased from 10% to 20%, the removal efficiency of TPAH increased. In addition, the removal efficiency of TPAH of the other two treatments tended to be stable after the dose increased. This may be since some organic pollutants are fixed by the soil particles, which prevents them from continuing to be oxidized,[39] and the application of excessive PAA and SPAN-20 can promote the PAHs desorption in soil particles and further degrade them through the KMnO$_4$ oxidation.

To explore the degradation effect of modified nZVI and KMnO$_4$ on LMW/MMW/HMW PAHs in soil, the 10% SE-nZVI treatment with the best TPAH degradation efficiency was selected, and the results are shown in the colored bar section of Fig. 6(b). Under the condition of KMnO$_4$ dosage of 40% SOD$_{max}$, the degradation efficiency of LMW/MMW/HMW PAHs in soil was significantly improved by applying 10% SE-nZVI, and the treatment efficiency was higher than 80%. It can be further seen from Fig. 6 that compared to the 10% SE-nZVI-KMnO$_4$ coupling system, the removal efficiency of PAHs by the un-optimized KMnO$_4$ single oxidation system and simple combined process of nZVI-KMnO$_4$ are 58.9% and 62%, respectively. Therefore, the surfactant-modified nZVI did greatly enhance the degradation effect of soil TPAH, and the optimal removal efficiency of the system is 1.3–1.5 times that of the un-optimized system. The removal efficiency of this system for LMW was the highest, reaching 85.6%, which has practical application value for remediating soil polluted by high ecological risk PAHs.

3.3 Degradation process and mechanism

To identify the degradation products of PAHs in the soil treated by the optimal coupled oxidation system ([SE-nZVI] = 10%, [KMnO$_4$] = 40% SOD$_{max}$), the extracts from the dry soil after treatment were analyzed by GC/MS full scan. The corresponding GC/MS chromatogram and the degradation products of PAHs are shown in Fig. 7. Three main peaks can be observed in the figure, which can be obtained by comparing with the MS standard database, and the peak at 20.74 min refers to the derivative of methylene fluorene (9-methylene-9H-fluorene, m/z: 178.08). The peak position at 29.01 min corresponds to fluoranthene (m/z: 202.08). The low peak value at 30.48 min refers to the ketone derivative of diphenylacetylene (1,5-diphenyl-1,4-pentadiyn-3-one, m/z: 230.26). Studies have shown that high molecular ketones, quinones, aldehydes, and furans in oxidized PAHs system have mutagenic and carcinogenic effects.[40–42] Therefore, it is necessary to pay attention to their ecological risks. The degradation products obtained in this study are all low-ring aromatic products, which can greatly reduce the environmental risks caused by HMW in the original contaminated soil.[43] Under the nZVI-KMnO$_4$ system, the soil TPAH content decreased overall. Therefore, it is speculated that after the treatment of nZVI-KMnO$_4$, the HMW/MMW in the soil gradually opens and cracks, resulting in a decrease in the ring number, forming a low-toxicity and high-hydrophilic LMW, which is further degraded by the oxidation reaction via ring-opening. After the reaction, three main degradation products of 1,5-diphenyl-1,4-pentadiyn-3-one, 9-methylene-9H-fluorene, and fluoranthene are generated. The oxidation mechanism of PAHs by KMnO$_4$ according to Clar's and Wang's research, which showed that PAHs are self contained a true carbon–carbon double bonds, stabilizing aromatic sextets and shared carbon–carbon double bonds. An increase in these bonds number results in an increase in reactivity except the stabilizing aromatic sextets, these factors make PAHs have a certain activity degree, which brings up the possibility of KMnO$_4$ to attack the aromatic rings.[38,49,50] Therefore, the interaction between KMnO$_4$ and PAHs may also be mainly electrophilic substitution reaction. As expected, these low-loop products that are eventually generated prove this view.

According to the reaction process and product analysis, the possible mechanism of nZVI-KMnO$_4$ treating soil PAHs was
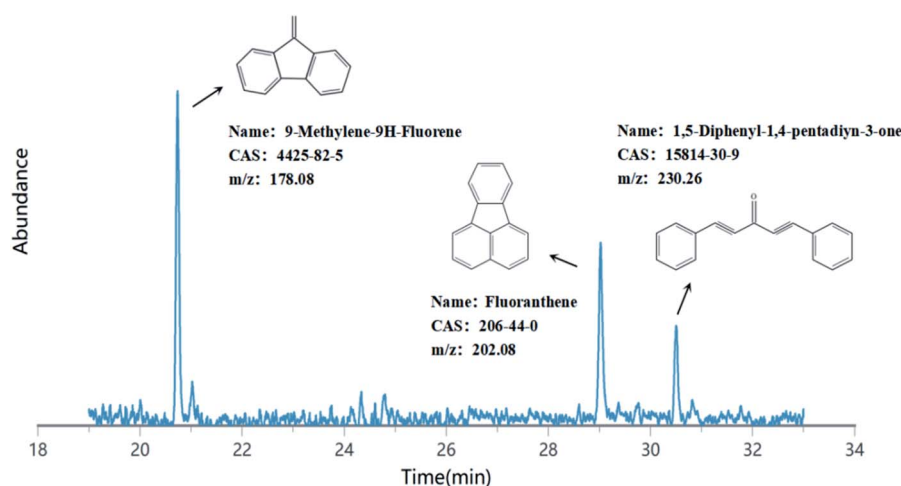

Fig. 7 Degradation of PAHs in soil by 10% SE-nZVI-KMnO$_4$ (40% SOD$_{max}$) extracted by GC/MS.

proposed, and the results are shown in Fig. 8. After the lipophilic PAHs enter the soil, some of them migrate to the vitreous organic matter to occur stably under the action of geophysical chemistry. Such PAHs are "locked" by the organic matter and are difficult to desorb from the adsorption site.[44,45] Some other PAHs enter into the submicron or nanoscale pores of the soil and it is difficult to migrate and transform.[46] These two parts of PAHs are called non-bioavailable PAHs and have little impact on the ecological environment. The last part of PAHs migration occurs in soil dissolved organic matter (DOM), including soil humus, rainfall eluent, microbial biomass, and root exudates, which are easily desorbed in water, acid, alkali, and salt solutions and migrate to the liquid phase system along with DOM.[47] Based on this, the degradation process of PAHs in the oxidation system was analyzed as follows: first of all, DOM in soil carried MMW/HMW PAHs with low water solubility (such as DBA, BaA) and LMW PAHs with high water solubility (such as PHE) to the liquid phase. Some LMW PAHs with high mobility could migrate directly to the liquid phase, which increases the probability of contact reaction between PAHs and oxidants. Secondly, in the oxidation system of $KMnO_4$, oxidants and catalytic particles are generated through ionization, electrophilic substitution reaction, redox, and catalytic reaction, which gather around DOM-coated PAHs and water-soluble LMW PAHs to provide oxidation reaction conditions.

Through the analysis of degradation mechanisms and products, it can be seen that in the $KMnO_4$ oxidation system (Fig. 8), $KMnO_4$ can directly oxidize PAHs existing on the surface

of DOM in solution to become intermediates. At the same time, manganese oxides (MnO_2, $MnOOH/Mn_2O_3$) and iron hydroxide ($Fe(OH)_3/FeOOH$) formed *in situ* enhance the further degradation of PAHs and intermediates through oxidation and adsorption. In addition, the *in situ* iron-manganese oxide ($MnFe_2O_4$) formed by the complexation or co-precipitation of dissolved $Mn(\text{II})$ with iron oxide promotes the adsorption of pollutants and can maintain the reactivity of nZVI through delayed passivation.[48] In conclusion, the PAHs in the soil eventually generate three main degradation products of 9-methylene-9*H*-fluorene, fluoranthene, and 1,5-diphenyl-1,4-pentadiyn-3-one through the oxidation of the $KMnO_4$ system.

4.   Conclusion

This study took 5% PAA, 20% SE and 10% SPAN-20 as dispersants to coat and modify nZVI to form a stable surface coating, which can effectively reduce the agglomeration of single nZVI and significantly improve its penetration performance and stability. In addition, taking $KMnO_4$ as an oxidant under 40% SOD_{max} can degrade 58.89% of TPAH in the soil. The results showed that the nZVI-$KMnO_4$ system possessed a better remediation effect on soil PAHs. Compared to the control group, the removal efficiency of TPAH and LMW/MMW/HMW PAHs was significantly improved after applying dispersants modified nZVI, especially after 10% SE was added, of which the removal efficiency of TPAH was as high as 85.0%. The 10% SE-nZVI-$KMnO_4$ also made the removal efficiency of LMW PAHs increase by 39% and finally reached 85.6%, which has practical application value for soil remediation with high PAHs ecological risk. Therefore, it is found that this non-toxic and easily biodegradable non-ionic surfactant—Sugar Esters (SE) used as a dispersant for the preparation of modified nZVI material is more suitable for coupling with $KMnO_4$ to form an oxidation system (SE-nZVI-$KMnO_4$), which has significantly improved the removal effect of PAHs in soil. The optimum conditions were determined: [SE-nZVI] = 10%, [$KMnO_4$] = 40% SOD_{max}, reaction at 25 °C for 24 hours. In addition, it was further speculated by GC-MS that adsorption and electrophilic substitution reactions are the oxidation mechanisms of SE-nZVI-$KMnO_4$ coupling system for the treatment of PAHs. After PAHs is oxidized and degraded, three main degradation products (1,5-diphenyl-1,4-pentadiyn-3-one, fluoranthene, 9-methylene-9*H*-fluorene) are finally formed. The above results will provide feasible ways for the preparation of nZVI composite materials with better performance on soil organic pollutant removal.

At present, most literature on the treatment of PAHs contaminated soil by chemical oxidation system focus on the high treatment effect, but its feasibility and economy in practical application are also very important. In this study, PAHs contaminated soil from industrial contaminated sites was used for effect research. Compared with previous research reports on pure treatment effects, it has more application value and applicability to specific organic contaminated site soil, and provides new insights in the field of ISCO. In general, this study provides new insights into the preparation of efficient nanomaterials and applicable technologies for remediation of PAHs contaminated soils.
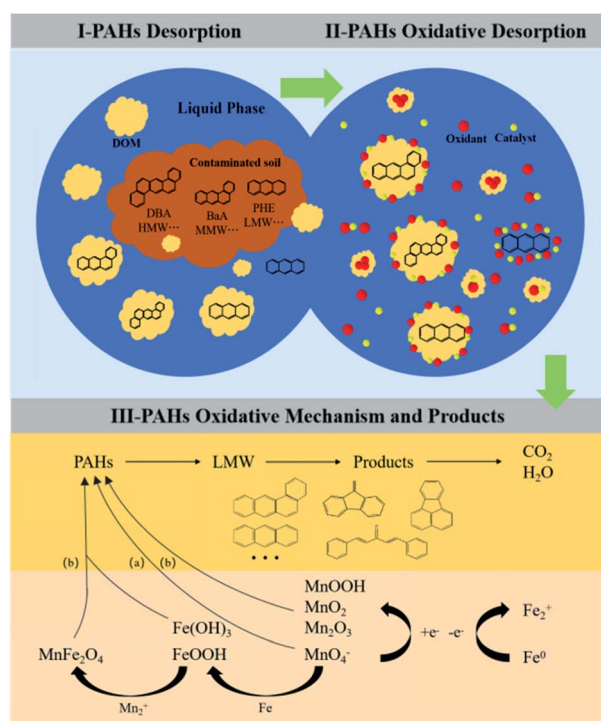

Fig. 8 Mechanism analysis of soil PAHs degradation by nZVI coupled with potassium permanganate system ([SE–nZVI] = 10%, [$KMnO_4$] = 40% SOD_{max}); Path (a) represents the free radical oxidation process of MnO_4^-; Path (b) represents the adsorption assisted oxidation process.

Abbreviations

nZVI	Nanoscale zero-valent iron
PAHs	Polycyclic aromatic hydrocarbons
$KMnO_4$	Potassium permanganate
POPs	Persistent organic pollutants
SPAN-20	Sorbitan monolaurate
PAA	Poly acrylic
SE	Sugar esters
SOD	Soil oxidation demand
SOD_{max}	Maximum soil oxidant demand
TPAH	Total PAH
LMW	Low molecular weight
MMW	Medium molecular weight
HMW	High molecular weight
DOM	Dissolved organic matter
ISCO	*In situ* chemical oxidation
BET	Specific surface area
HPLC	High-performance liquid chromatography
GC-MS	Gas chromatography-mass spectrometry
XRD	X-ray diffraction
SEM	Scanning electron microscope

Author contributions

All authors contributed to the study conception and design. Material preparation, data collection and analysis were performed by Xiaoshuang Sun, Yuerong Wu, Zongxin Ran, Chengwei Zhong, Weiwei Zhu, Hameed Hllah and Jiang Yu. The first draft of the manuscript was written by Xiaoshuang Sun and all authors commented on previous versions of the manuscript. All authors read and approved the final manuscript.

Conflicts of interest

There are no conflicts to declare.

Acknowledgements

Notes and references

1 D. Zhao, X. Y. Liao, X. L. Yan and Z. Y. Chong, *Environ. Sci.*, 2011, **32**(03), 857–863.

2 Q. Chen, W. Cai, J. Chen, H. B. Zhao, L. I. Chang-Xin and H. E. Yun-Feng, *J. Zhejiang Univ., Sci., A*, 2019, **53**(12), 2437–2444.

3 R. A. Crane and D. J. Sapsford, *Chem. Eng. J.*, 2018, **345**, 126–137.

4 C. Goring, D. A. Laskowski, J. W. Hamaker and R. W. Meikle, Principles of Pesticide Degradation in Soil, *Environmental Dynamics of Pesticides*, 1975.

5 Y. Li, Y. Xiao, X. Li and C. Yang, *Acta Sci. Circumstantiae*, 2015, **35**, 499–507.

6 H. Qiang, MD thesis, Taiyuan University of Technology, 2016.

7 W. Yi, MD thesis, Zhejiang University, 2015.

8 C. Xi, MD thesis, Zhejiang University, 2014.

9 L. Kan and Z. Liu, *Environ. Sci. Technol.*, 2019, **42**(06), 215–223.

10 X. Yang, Y. Wang and L. I. Minrui, *Chem. Ind. Eng. Prog.*, 2019, **38**(07), 3412–3424.

11 J. He, X. Y. Wang, P. Wang and K. Q. Liu, *Environ. Sci.*, 2015, **36**, 980–988.

12 Y. H. Lin, M. Lin and C. Liang, *presented in part at the Chemical, Biological and Environmental Engineering – The International Conference on CBEE 2009*, 2010.

13 Q. Wang, Y. Kuang, X. Jin and Z. Chen, *Acta Sci. Circumstantiae*, 2014, **34**, 1228–1235.

14 M. Basnet, S. Ghoshal and N. Tufenkji, *Environ. Sci. Technol.*, 2013, **47**, 13355–13364.

15 C. H. Xu, L. J. Zhu, X. H. Wang, L. Sheng and Y. M. Chen, *Water, Air, Soil Pollut.*, 2014, **225**, 1845.

16 Q. Yin, L. I. Xiaoqin, L. I. Ying and Y. Xiao, *Chem. Ind. Eng. Prog.*, 2013, **32**(7), 1598–1603.

17 H. T. Zhang, W. J. Liu, Y. Liu, F. U. Ling-Zi and M. Y. Kou, *Guangzhou Chem. Ind.*, 2019, **13**, 30–32.

18 Z. Fang, X. Qiu, J. Chen and X. Qiu, *J. Hazard Mater.*, 2011, **185**, 958–969.

19 Y. P. Sun, X. Q. Li, J. Cao, W. X. Zhang and H. P. Wang, *Adv. Colloid Interface Sci.*, 2006, **120**, 47–56.

20 L. U. Yin-Tao, X. Xiang, S. C. Zhang, M. L. Liu, J. Wang, L. I. Shuang, H. Yao and S. B. Sun, *Environ. Sci.*, 2019, **7**, 178–184.

21 R. Lohmann, J. K. Macfarlane and P. M. Gschwend, *Environ. Sci. Technol.*, 2005, **39**, 141–148.

22 Y. Yang, J. Zhang, K. Chen, Z. Li and Y. Wang, *Chin. J. Environ. Eng.*, 2016, **10**, 427–431.

23 L. Yu-Hao, T. Hui-Hsin, W. Ming-Yen and L. Min-Der, *Colloids Surf. A Physicochem. Eng. Asp.*, 2009, **349**, 137–144.

24 W. Ran, X. Xinghui and M. Lihong, *Environ. Sci.*, 2006, **27**, 855–861.

25 L. Martin-Neto, D. G. Traghetta, C. M. P. Vaz, S. Crestana and G. Sposito, *J. Environ. Qual.*, 2001, **30**, 1101–1103.

26 L. N. Shi, Z. Xin and Z. L. Chen, *Water Res.*, 2011, **45**, 886–892.

27 W. Wei, PhD thesis, Nankai University, 2008.

28 V. Drits, *Clay Clay Miner.*, 1997, **45**, 461–475.

29 E. Ferrarese, G. Andreottola and I. A. Oprea, *J. Hazard Mater.*, 2008, **152**, 128–139.

30 C. Sirguey, P. Silva, C. Schwartz and M. O. Simonnot, *Chemosphere*, 2008, **72**, 282–289.

31 B. W. Bogan and V. Trbovic, *J. Hazard Mater.*, 2003, **100**, 285–300.

32 X. Liao, Z. Dan and X. Yan, *J. Hazard Mater.*, 2011, **193**, 164–170.

33 C. Wu, MD thesis, Zhejiang university, 2016.

34 I. D. Bossert and R. Bartha, *Bull. Environ. Contam. Toxicol.*, 1986, **37**, 490–495.

35 J. Lemaire, F. Laurent, C. Leyval, C. Schwartz, M. Bues and M. O. Simonnot, *Chemosphere*, 2013, **91**, 406–414.

36 W. Hao, PhD thesis, Shenyang University, 2017.

37 Y. J. Shih, N. T. Binh, C. W. Chen, C. F. Chen and C. D. Dong, *Chemosphere*, 2016, **150**, 294–303.

38 W. Wenchao, L. Gang, S. Jun, C. Honghong, L. Ruifeng, D. Jiankui, Y. Zhifeng and X. Qingbai, *J. Environ. Chem. Eng.*, 2015, **3**, 1513–1521.

39 W. Chunyan, MA thesis, Beijing University of Chemical Technology, 2012.

40 B. Bandowe, J. Sobocka and W. Wilcke, *Environ. Pollut.*, 2011, **159**, 539–549.

41 M. Bergknut, A. Kitti, S. Lundstedt, M. Tysklind and P. Haglund, *Environ. Toxicol. Chem.*, 2004, **23**, 1861–1866.

42 W. Xue and D. Warshawsky, *Toxicol. Appl. Pharmacol.*, 2005, **206**, 73–93.

43 Z. Cancan, MD thesis, University of Chinese Academy of Sciences, 2013.

44 U. Ghosh, J. W. Talley and R. G. Luthy, *Environ. Sci. Technol.*, 2001, **35**, 3468–3475.

45 K. Nam, N. Chung and M. Alexander, *Environ. Sci. Technol.*, 1998, **32**, 3785–3788.

46 L. Qi-shi, Z. Xi-hui, W. Hui and Q. Yi, *The ecological environment*, 2004, **13**, 3.

47 L. Shaosheng and D. Youxin, *Jiangxi Forestry Science and Technology*, 2010, 23–26.

48 X. Wang, L. Le, A. Wang, H. Liu, J. Ma and M. Li, *J. Taiwan Inst. Chem. Eng.*, 2016, 115–125.

49 G. S. Brown, L. L. Barton and B. M. Thomson, *Waste Manag.*, 2003, **23**, 737–740.

50 E. Clar, The Significance of Double Bonds and Kekulé Structures for the Stability of Aromatic Systems, *Polycyclic Hydrocarbons*, 1964.